LANDSAT-4 SENSOR PERFORMANCE

by

John L. Barker

Earth Resources Branch/Code 923
NASA/GODDARD SPACE FLIGHT CENTER
Greenbelt, MD 20771
(301) 344-8978 or 344-8308

and

Fred J. Gunther
Staff Scientist
Earth Observations Systems Department
COMPUTER SCIENCES CORPORATION (CSC)
8728 Colesville Road
Silver Spring, MD 20910
(301) 589-1545

Presented at

Pecora VIII
The Eighth Williams T. Pecora Memorial
Remote Sensing Symposium
Sioux Falls, South Dakota

on

October 4, 1983

NAS5-24350

ABSTRACT

The new Earth resources satellite, Landsat-4, has multispectral scanner (MSS) sensors to provide continuity of 80m, 4-band, image data and thematic mapper (TM) sensors to provide experimental, 30m, 7-band image data. In the TM, familiar Landsat spectral bands are narrower, more sensitive, and more sharply defined; new spectral bands extend instrument range into blue/green and thermal infrared regions.

Preflight and in-orbit sensor and data measurements indicate that TM meets or exceeds most specifications. Measured spectral band edges meet instrument specifications in 12 out of 14 cases. Typical scenes do not saturate either high or low counts, so there is ample dynamic range. The signal-to-noise ratio (SNR) exceeds specifications, except for band 3, channel 4; band 7 channel 7 is very noisy but still meets specifications. The modular transfer function (MTF) of channel 4, band 2, is smaller than specified; the suspect data is currently being replaced by data from channel 5. Registration errors between the primary focal plane (PFP) and the cold focal plane (CFP) are about 0.75 pixels along-scan and 0.2 pixels across scan. Forward and reverse scan discontinuities, due to attitudinal deviations (jitter), are well within ground-processing capabilities to rectify. Instrument gain variability, up to 7% for band 5, requires use of the internal calibration (IC) system to assure radiometric accuracy.

Preliminary applications evaluation of image contents indicates that TM provides much better definition of edges than MSS. Detailed ground truth permits pixel-by-pixel location of ground features: individual large buildings, parking lots, small lakes, grass lawns, etc. Differences in roof material and orientation can be detected. Differences in forest types can be mapped.

TABLE OF CONTENTS

INTRODUCTION

This paper discusses some aspects of sensor performance of NASA's Landsat-4, the newest Earth resources satellite. Launched on 16 July 1982, the satellite's two sensor systems provide two types of digital images of the surface of the Earth. The two sensing systems are the payload for the Multimission Spacecraft (MMS), which features modular design and is potentially retrievable using the shuttle transportation system (STS) (Salomonson & Park, 1979). The multispectral scanner (MSS) provides data continuity with previous Landsat satellites (Engel et al., 1983). Thematic mapper (TM) is a new experimental system which is being evaluated as a possible replacement for MSS-type systems. Images were acquired starting three days after launch by MSS. Higher resolution 4-band TM images were acquired starting a day later; full 7-band TM images were acquired starting in late August.

The TM sensor is designed to provide increased spectral, radiometric, and geometric performance (Engel et al., 1983). The primary improvement of TM over MSS is in spatial resolution (Salmonson & Park, 1979). Each TM pixel represents a 30m area on the ground, instead of 80m for MSS. A second major improvement is in new and more precisely located spectral bands. Finally, TM has higher radiometric resolution, namely 8-bit precision as compared to 6-bit for MSS. These improvements are expected to provide many new and improved capabilities (Salmonson & Park, 1979; Covault, 1982a), including: 1) mapping of coastal water areas to water depths of 20-40 meters; 2) differentiation between soil and vegetation; 3) biomass surveys; 4) differentiation between coniferous and deciduous vegetation; 5) differentiation between plant species; 6) differentiation between clouds and snow cover; 7) discrimination of hydrothermal alteration zones in rock units; 8) differentiation between soil and vegetation; and 9) studies of plant heat stress and rock-unit thermal characteristics. Preliminary evaluations indicate that TM image products are "beyond expectations" (Covault, 1982a and 1982b), with "... spectral and spatial detail clearly surpassing that provided by ... MSS" (Salmonson & Koffler, 1983).

Prior to the transfer of operational responsibility for TM from NASA to NOAA in January 1985, digital imagery acquired from the TM sensor will be scientifically investigated from two perspectives. Firstly, there is a spectral, radiometric and geometric characterizaton of how well the radiance is being measured. This program is underway at NASA's Goddard Space Flight Center. A multinational Landsat-4 Early Results Symposium was held on February 22-24, 1983 to provide an initial review of images from both MSS and TM sensors. Secondly, a program has been started to identify and quantify the scientific variables that can be derived for various applications of this measured radiance. A parallel engineering evaluation of Landsat-4's performance is verifying its specifications and reliability. This paper concentrates on the performance of the TM sensor, its imagery and its potential information content. Lesser attention is paid to the performance of the MSS.

MEASUREMENT OF RADIANCE

Radiance may be characterized using three areas of investigation: spectrometry, radiometry, and geometry. Spectrometry considers the wavelength-dependent aspects of radiance; e.g., where are the bands located and what is the relative variability of the band widths and band edges? Radiometry is a measure of the intensity of the reflected and emitted radiance as a function of time. Geometry deals with radiance as a function of location, both size and position.

Spectral Characterization

Spectral specifications for sensors determine what can be inferred from imagery by defining where to look in the electromagnetic spectrum. Landsat-4 MSS characteristics have been published earlier (Markham & Barker, 1983b). TM has six bands which respond to reflected light and one band for measuring thermally emitted radiance. Compared with MSS, TM

bands are more sharply defined, more sensitive, and sample a wider range of the electromagnetic spectrum (Williams, 1983).

The filters for each TM band were tested before launch at the Hughes Santa Barbara Research Center (SBRC) to determine the relative spectral response curve as a function of wavelength. From these curves, the exact locations of the top and bottom edges of each spectral band were determined. Defined as the spectral location where instrument response is half of the maximum response, the measured band edges meet instrument specifications in 12 out of 14 cases (Table 1). The upper band edge for band 5, 1784nm versus 1750nm, may allow a greater than expected influence of atmospheric water vapor on the instrument measurements. The upper band edge for band 6, 11.6 microns, provides a narrower window than specified; this is not critical because the sensor radiometric response was significantly better than specified (Markham & Barker, 1983a).

Radiometric Characterization

Dynamic Range

The TM analog-to-digital converter is designed to provide a range of 0 to 255 digital numbers (DNs) or counts. This is four times the dynamic range or number of grey levels of MSS data (Williams, 1983) and eight to 12 times the number of grey levels that the human eye can discriminate (Moik, 1980, p. 128). Histograms of typical scenes indicate that bands 1, 2, 3, 6, and 7 do not utilize the available dynamic range as well as do bands 4 and 5 (Barker, 1983a). Research by the authors indicates that even scenes with snow (bright) and water (dark) produce saturated pixels only for band 1; the utilized range in DNs for the respective bands is 65-255, 26-177, 27-209, 19-165, 2-96, 65-96, and 0-61, if presumed specular-reflection pixels are omitted.

LANDSAT-4 TM SPECTRAL CHARACTERISTICS

OBSERVED BAND LOCATIONS (NANOMETERS (NM) AT HALF MAXIMUM)

BAND	LOWER BAND EDGE	UPPER BAND EDGE	BANDWIDTH
1	452	518	66
2	529	610	81
3	624	693	69
4	776	905	129
5	1568	1784*	216
7	2097	2347	250
6 (μm)	10.422	11.661*	1.239

*OUT OF SPECIFICATION CHARACTERISTICS

Table 1. Landsat-4 TM Band Spectral Locations (After Markham & Barker, 1983a).

MSS Coherent Noise

Images and digital data have exhibited a diagonal striping patterm (Rice, 1983). This coherent noise (Figure 1) has been reduced by a process of resequencing the data back into the telemetry sequence of minor frames, taking a Fourier transform and developing a notch filter. After the notch filter is applied to the Fourier transform image, an inverse Fourier transform restores the image with coherent noise reduced (Figure 2).

TM Signal-to-Noise

Prelaunch testing also determined TM radiometric sensitivity. The signal-to-noise ratio (SNR) is defined, for "... a constant input radiance, ... as the ratio of the output value (in units of radiance) averaged over at lease 100 samples to the root mean square (RMS) value of the noise equivalent radiance which is defined as the RMS of the deviations of the output samples from the average value" (Weinstein & Banks, 1978). The SNR of the TM meets specifications except in the case of band 3, channel 4 (Table 2; Barker et al., 1983b). In addition, band 7, channel 7, has a SNR about half that of the next lowest channel.

"Noise" can have several sources. "Droop" is the change in gain from one end of a scan line to the other (Figure 3). "Bright-target recovery" problems arise if clouds occupy a major portion of one side of a scene. "Channel-correlated noise" derives from the optics and electronics that produce each data channel. Measured values of each type of noise indicates that they are minor influences on image data (Table 3).

Table 2. Signal-to-Noise Ratio (SNR) data for TM reflective bands.

LANDSAT-4 THEMATIC MAPPER

SIGNAL-TO-NOISE RATIO (SNR)

BAND	MINIMUM SATURATION LEVEL RADIANCE	
	SPECIFIED	OBSERVED
1	85	152
2	170	281
3	143	235
4	240	341
5	75	180
7	45	175

Speculative Radiometric Assignments

Landsat-4 TM/PF
Band 1 Channel 4

Cause	Label	Magnitude* (DN)
Droop	D	.4
Bright Target Recovery	B	1.0
Channel-Correlated Noise	N	2.0

* Based on Analysis of Shutter collects Before and After DC Restoration for Landsat Scene 40174-16011 WRS:P022R040 - 3 January 1983 Terrebonne Bay, LA with Clouds on Bottom and East

Table 3. Results of One Analysis of Noise Content.

TM Calibration

TM image within-band calibration data is collected by letting all channels sense the internal calibration (IC) during the mirror-reversal time at the end of each sweep (Engel, 1980). Pre-launch data for the IC system indicates that average pulse value in digital counts has an extremely linear relationship with the number and brightness of calibration lamps (Figure 4). The IC system was calibrated before launch using pre-launch characteristics of the TM channels as determined by pre-launch testing at SBRC (Barker et al., 1983b; Engel et al., 1983).

The application of radiometric calibration to image data is done in the ground processing segment. Different portions of the IC pulse scan are measured for each lamp state (Figure 5). The pulse width in the ground processing software can be changed; the Hughes algorithm uses 30 minor frames (Figure 6), but the TM Image Processing System (TIPS) at Goddard uses a 64 minor-frame pulse-average width. Parametric analytical runs using the TM Radiative and Algotithmic Performance Program (TRAPP) program developed by Computer Sciences Corporation (CSC) on the standard deviation of the pulse value for different pulse integration widths indicates that the pulse value does not stabilize at narrow widths (Figure 7). A large pulse integration width can produce a factor of two reduction in pulse variability, especially for IC lamp configurations involving lamp 2 or band 4 on the TM. In addition, lamp configuration 111 (all on) should not be used in TM band-4 calibration because of saturated (DN=255) calibration pulse pixels.

The standard calibration procedure (Figure 8) takes the DNs for each channel and applies the internal calibration data for each channel of data. The data corrected by the IC procedure is then processed by histogram equalization procedures to produce the calibrated image (Table 4).

POST-LAUNCH RADIOMETRIC CALIBRATION OF LANDSAT TM TO UNIFORM GAIN AND OFFSET FOR EACH CHANNEL WITHIN A BAND

BAND NUMBER	RMIN (AT Q = 0 DN)	RMAX (AT Q = 255 DN)
	($mWcm^{-2}sr^{-1}\mu m^{-1}$)	($mWcm^{-2}sr^{-1}\mu m^{-1}$)
1	-0.152	15.842
2	-0.284	30.817
3	-0.117	23.463
4	-0.151	22.432
5	-0.037	3.242
7	-0.015	1.700

N.B. RMIN IS THE LARGEST MINIMUM RADIANCE OBSERVED IN THE BAND.
RMAX IS THE SMALLEST MAXIMUM RADIANCE OBSERVED IN THE BAND.
KG = GAIN AFTER CALIBRATION = 255/(RMAX-RMIN)
KO = OFFSET AFTER CALIBRATION = 255 - (KG*RMAX)

Table 4. Landsat-4 TM Gain and Offset.

Differences between the products of the two types of calibration, nominal followed by histogram equalization and IC followed by histogram equalization, were investigated by producing difference images for corresponding bands of the CCT-AT images. The difference images (Figure 9) and Barker et al., 1983c) show that : 1) DN differences between the two calibration techniques are almost always less than 2 DN levels; 2) not all lines have calibration changes, a result of integer arithmetic; 3) some detectors produce similar DN differences; 4) patterns of DN differences are different in forward and reverse sweeps; and 5) each TM band has its own pattern of changes in calibration.

Gain Stability

The IC system of the TM instrument was used to measure the change in gain over time (Barker et al., 1983b). For the primary focal plane (PFP), the gain exhibits an apparent exponential decrease (Figure 10). Because the cold focal plane (CFP) was not turned on as soon after launch as the PFP, exponential decay is not observed, but considerable change (Figure 11) and cyclic variability (Figure 12) are observed. Variations in thickness of water ice is suspected of blocking light reception (Figure 13), especially because of the return to more normal gain values after instrument outgassing in January 1983.

It is essential to apply IC radiometric calibration procedures before any histogram equalization procedures, so that both relative and absolute interband and interchannel radiometric accuracy may be preserved.

Geometric Characterization

An understanding of image geometry characteristics facilitates image use not only within the boundaries of a single image but also in the generation of precise multi-image overlays and wide-area mosaics (Moik, 1980, p. 199-200). Within each multispectral image, the individual bands must be registered to

each other within known and acceptable limits; the registration must be capable of improvement by computer processing for special cases.

Between Focal-Plane Band Registration

The TM optical path has two focal planes. The detectors for the visible and low infrared spectral bands (bands 1-4) require a different thermal environment than the detectors for the higher reflected infrared and thermal infrared (bands 5-7) (Engel, 1980; Covault, 1982a). Examination of image data has shown that the PFP to CFP misregistration is 0.75 pixels along-scan and 0.2 pixels across scan (Barker, 1983a).

Scan Underlap/Overlap

In the very short time needed for the scanner mirror to reverse direction, attitudinal deviations can cause the sensor to point in a direction slightly different from that expected. Average overlap (double coverage) for 20 scenes for the reflective bands ranges from -0.326 pixels to -0.345 pixels; average underlap (missing coverage) ranges from 0.356 to 0.360 pixels. Roll attitude deviation can produce scan discontinuities that range from zero to twice the roll attitude deviation, depending upon the phase relationship of the scan mirror and the attitude deviation. Scan discontinuities of nearly one pixel have been observed in some scenes during loss of payload correction data (PCD). Ground processing use of PCD permits correction of scan discontinuities by interpolation, to form final geometrically-correct images (Barker, 1983a).

Within Scan Vibrations

Deviations in spacecraft attitude have been measured in

orbit to determine if interactions between different operating systems (TM, MSS, and antenna drive) affect the image quality of the TM (Covault, 1982a). Attitude deviations, measured by the angular displacement sensor (ADS) on the TM when the MSS is operating, are found at frequencies of 7, 21, 35, 49, 63, 77, 91, 105 and 199 Hertz; amplitudes vary from 20 microradians in roll, through 10 in yaw to 5 in pitch. When TM is operating alone, the amplitude values are 15, 5, and 3. Effects of the antenna drive are under investigation (Barker, 1983a).

The observed attitudinal deviations are less than 0.5 pixels, and are correctable. The measured value of 20 microradians is much less than the ground processing limits; NASA ground processing has been validated at 200 microradians deviation during prelaunch testing (Barker, 1983a).

Modulation Transfer Function

The modulation transfer function (MTF) (Moik, 1980, p. 24) of band 2, channel 4, is smaller than specified. The suspect data was replaced in ground processing by the SCROUNGE system by data from channel 5, prior to cubic convolution resampling (Barker, 1983a).

APPLICATIONS OF MEASURED RADIANCE

Radiance measurements are usually reconstructed into images for use as photoproducts and as digital data. The former are processed into information products by photointerpretation; the latter by computer-assisted manipulation of the DNs for each band taken separately and together (Podwysocki et al., 1977).

Spectral and Radiometric Information

Urban areas are very diverse. Even an institution that covers as much ground as NASA/Goddard has very few pure TM pixels representing uniform ground cover (Figure 14).

Geometric Information

In the short time since launch of Landsat-4 and the turning on of the TM, it has not been possible to evaluate properly the full utility of TM image data to all scientific areas of investigation. A comparison of images for the same area of the Washington D.C. beltway examined at the same scale show the following TM advantages:

- Smoother linear boundaries, resulting from smaller pixel size and thus a larger number of pixels per unit area on the ground, and resulting from cubic convolution resampling that provides a smoothing effect.
- better definition of residential street patterns.
- better definition of agricultural field boundaries.
- better definition of small water bodies, including water hazards in a golf course.
- better definition of location and shape of large buildings.

Detailed photointerpretation of digitally enlarged and color-coded TM image segments centered on NASA/Goddard permits pixel by pixel location of ground features. Forest versus built-up areas can be seen; subtle variations within the forest indicate pine, broad-leaf, and mixed forest types. The bare dirt of a construction site can be located, as well as Goddard Lake. Many building locations are obvious (Figures 15 and 16), and all can be found. Some parking lots and grass lawns can be discriminated. In the complete set of images, not only can all buildings be located, but also reflectance differences due to roof material and orientation can be detected.

DISCUSSION

Information flow from digital Landsat images can be viewed in four parts: 1)observation, 2) calibration to inferable variables, 3) information extraction, and 4) use. This paper has delt primairly with an overview of the steps in going from observed raw digital counts of radiance to calibrated values of spectral radiance. Future work will presumably be concerned with directional reflectance or albedo for atmospheric and non-atmospheric components. Information extraction techniques were used in applying ERIM linear spectral transformations to TM imagery to illustrate spatial information on pure and mixed pixels. The development of spatial/spectral information extraction algorithms remains as a priority item for future work on identification of point, linear, extensive and intensive areal, three-dimensional, and temporal features. Operational use of TM imagery cannot be expected until information extraction techniques have been developed for digital data of this type and resolution.

ACKNOWLEDGEMENTS

Data analyses were assisted greatly by the use of the TRAPP software. The TRAPP program was designed and implemented by Dr. R. Abrams (CSC), D. Ball (CSC), and B. Jeffe (CSC). We also thank B. Jeffe, S. Korfanty, C. Eldridge, and J. L. Wang of CSC for keeping track of tapes, data books, and computer runs. B. Jeffe produced program documentation and a Users Guide.

REFERENCES

1983a Barker, J. L., "TM Report," ABSTRACTS OF LANDSAT-4 EARLY RESULTS SYMPOSIUM, NASA/GODDARD SPACE FLIGHT CENTER, Greenbelt MD. 22-24 February 1983.

1983b Barker, J. L., D. L. Ball, K. C. Leung, & J. A. Walker, "Prelaunch Absolute Radiometric Calibration of the Reflective Bands on LANDSAT-4 Protoflight Thematic Mapper," ABSTRACTS OF LANDSAT-4 EARLY RESULTS SYMPOSIUM, NASA/GODDARD SPACE FLIGHT CENTER, Greenbelt MD. 22-24 February 1983.

1983c Barker, J. L., F. J. Gunther, R. B. Abrams, & D. L. Ball, "TM Digital Image Products for Applications," PROCEEDINGS OF THE LANDSAT-4 EARLY RESULTS SYMPOSIUM, NASA/GODDARD SPACE FLIGHT CENTER, Greenbelt MD. 22-24 February 1983.

1982a Covault, C., "Landsat D to Yield More Precise Data," AVIATION WEEK AND SPACE TECHNOLOGY, 5 July 1982, Pages 40ff.

1982b Covault, C., "Images from Space Reshape NASA Plans," AVIATION WEEK AND SPACE TECHNOLOGY, 7 August, 1982. Pages 16-18.

1980 Engel, J. L., "Thematic Mapper - An Interim Report on Anticipated Performance," CONFERENCE ON SENSOR SYSTEMS FOR THE 80'S," AMERICAN INSTITUTE OF AERONAUTICS AND ASTRONAUTICS, Colorado Springs CO. December 1980.

1983 Engel, J. L., J. C. Lansing, Jr., D. G. Brandshaft, & B. J. Marks, "Radiometric Performance of the Thematic Mapper," PROCEEDINGS, 17TH INTERNATIONAL SYMPOSIUM ON REMOTE SENSING OF THE ENVIRONMENT, Ann Arbor MI. May 9-13, 1983.

1983a Markham, B. L., & J. L. Barker, "Spectral Characterization of the Landsat Thematic Mapper Sensors," ABSTRACTS OF LANDSAT-4 EARLY RESULTS SYMPOSIUM, NASA/GODDARD SPACE FLIGHT CENTER, Greenbelt MD. 22-24 February 1983.

1983b Markham, B. L., & J. L. Barker, "Spectral Characterization of the Landsat-4 MSS Sensors," PHOTOGRAMMETRIC ENGINEERING AND REMOTE SENSING, Vol. 48, no. 6, June 1983. Pages 811-833.

1980 Moik, J., "Digital Processing of Remotely Sensed Images," NASA SPECIAL PUBLICATION 431, Washington D.C., 330 Pages.

1977 Podwysocki, M. H., F. J. Gunther, & H. W. Blodget, "Discrimination of Rock and Soil Types by Digital Analysis of Landsat Data," NASA/GODDARD SPACE FLIGHT CENTER, Document X-923-77-17. January 1977.

1983 Rice, D. P., "Investigation of Radiometric Properties of Landsat-4 MSS," ABSTRACTS OF LANDSAT-4 EARLY RESULTS SYMPOSIUM, NASA/GODDARD SPACE FLIGHT CENTER, Greenbelt MD. 22-24 February 1983.

1979 Salomonson, V. V., & A. B. Park, "An Overview of the Landsat-D Project with Emphasis on the Flight Segment," PROCEEDINGS OF THE FIFTH SYMPOSIUM ON MACHINE PROCESSING OF REMOTELY SENSED DATA, Purdue University, Lafayette IN. June 27-29, 1979.

1979 Salomonson, V. V., & R. Koffler, "An Overview of Landsat-4 Status and Results from Thematic Mapper Data Analysis," SUMMARIES, 17TH INTERNATIONAL SYMPOSIUM ON REMOTE SENSING OF THE ENVIRONMENT, Ann Arbor MI. May 9-13, 1983.

1978 Weinstein, O., & G. Bank, "GSFC Specifications, Thematic Mapper System and Associated Test Equipement," NASA/GODDARD SPACE FLIGHT CENTER, Document Number GSFC 400.8-D-201, Revision B, April 1978.

1983 Williams, D., "Landsat-4 Highlights," ABSTRACTS OF LANDSAT-4 EARLY RESULTS SYMPOSIUM, NASA/GODDARD SPACE FLIGHT CENTER, Greenbelt MD. 22-24 February 1983.

16 Unsupervised Clusters of "ISOCLASS"

North Carolina Subscene
Before Applying a Digital Notch Filter

(24 Sep 82, ID 40070-15081)

Alford/Barker/Tilton Sep 83

Figure 1. Landsat-4 MSS "with Noise" Classification Image.

Landsat-4
MSS

Radiometric
Precision

16 Unsupervised Clusters of "ISOCLASS"

North Carolina Subscene
After Applying a Digital Notch Filter

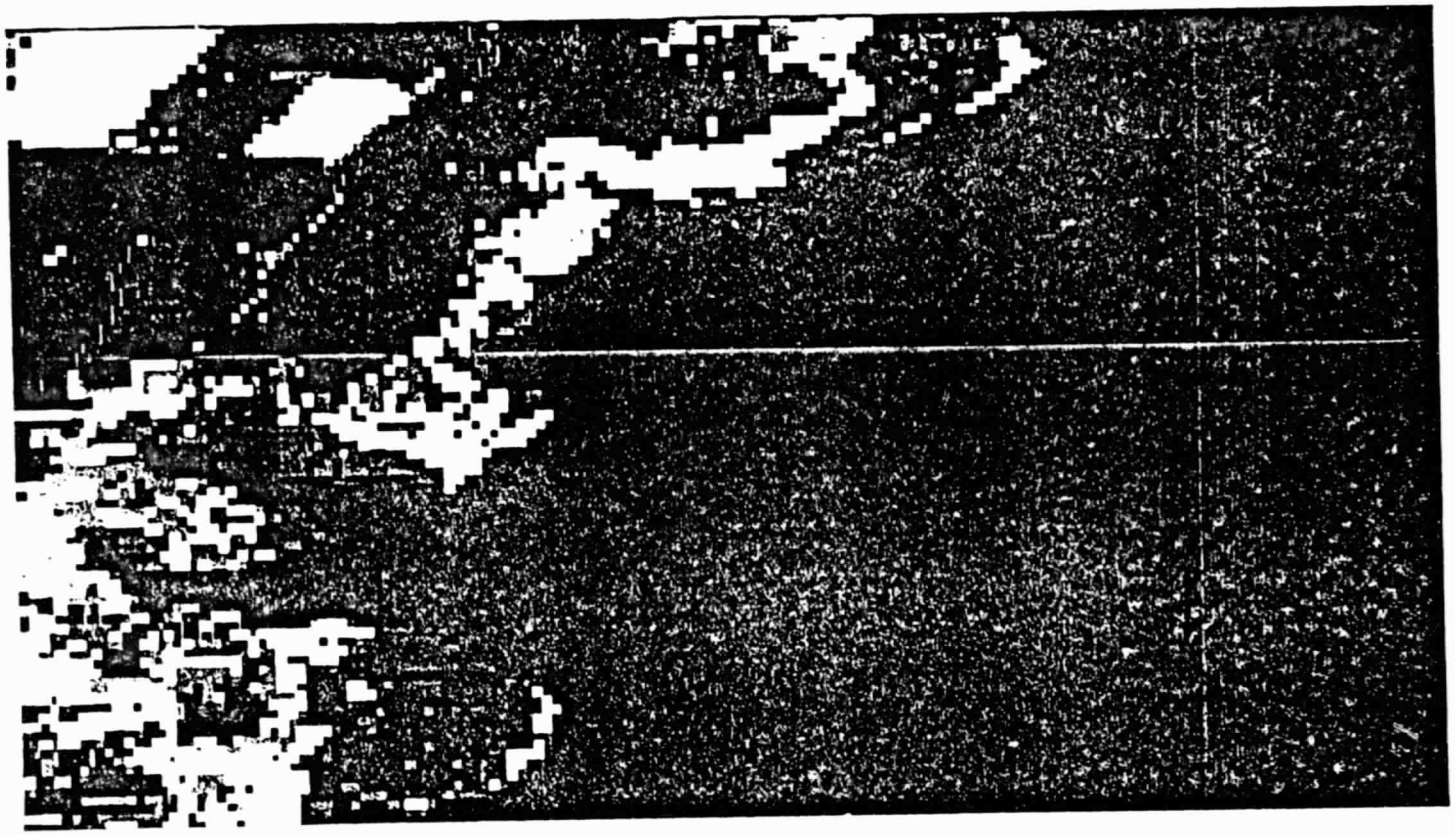

Alford/Barker/Tilton Sep 83

Figure 2. Landsat-4 MSS "without Noise" Classification Image.

POSTLAUNCH TM LANDSAT-4 RADIOMETRIC CALIBRATION

BETWEEN-LINE VARIABILITY OF IC PULSE
TM4, CHANNEL 9, LAMP 100, D.C., NOVEMBER 2, 1982

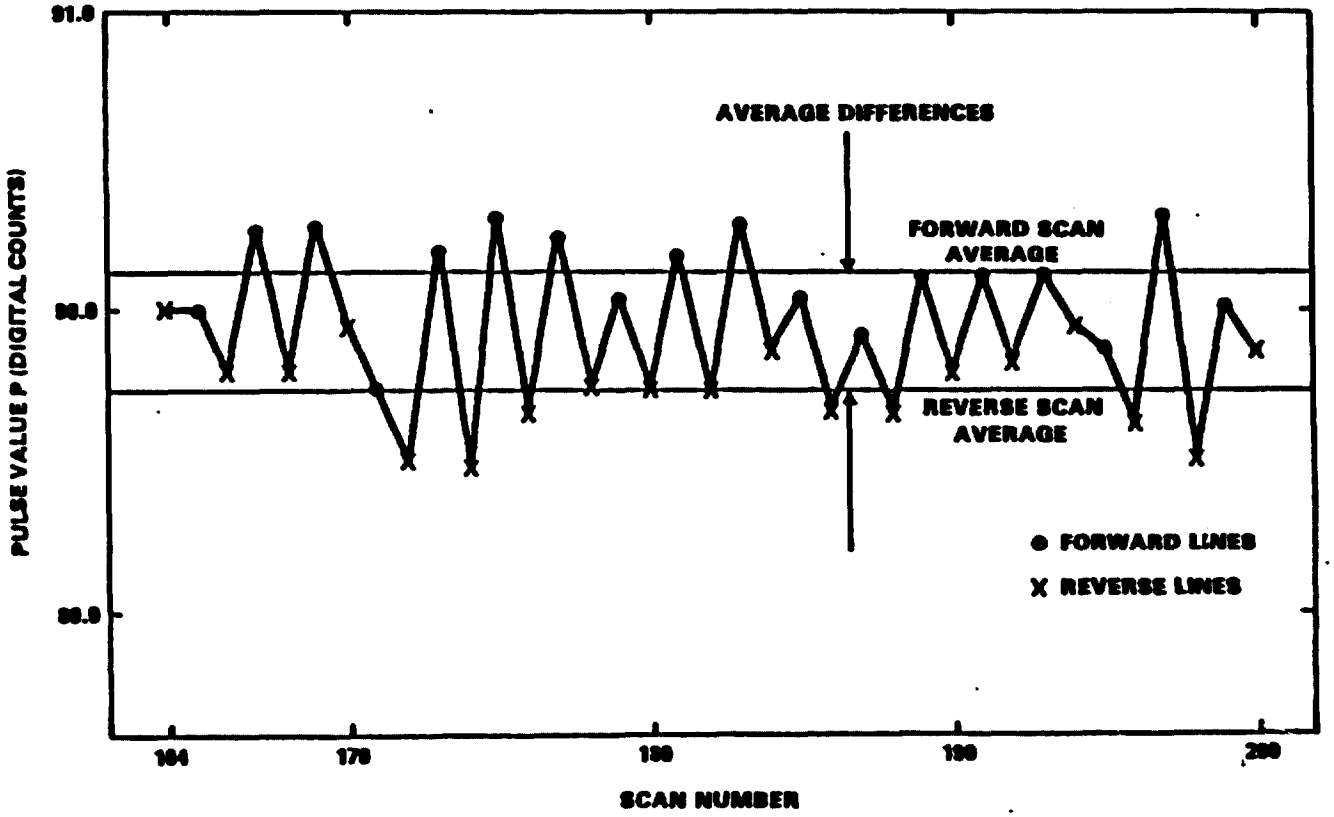

EXPECTED
DROOP

FWD-REV= D

Δ = 90.15
-89.8

.35

Figure 3. Landsat-4 TM Measured "Droop" in Gain.

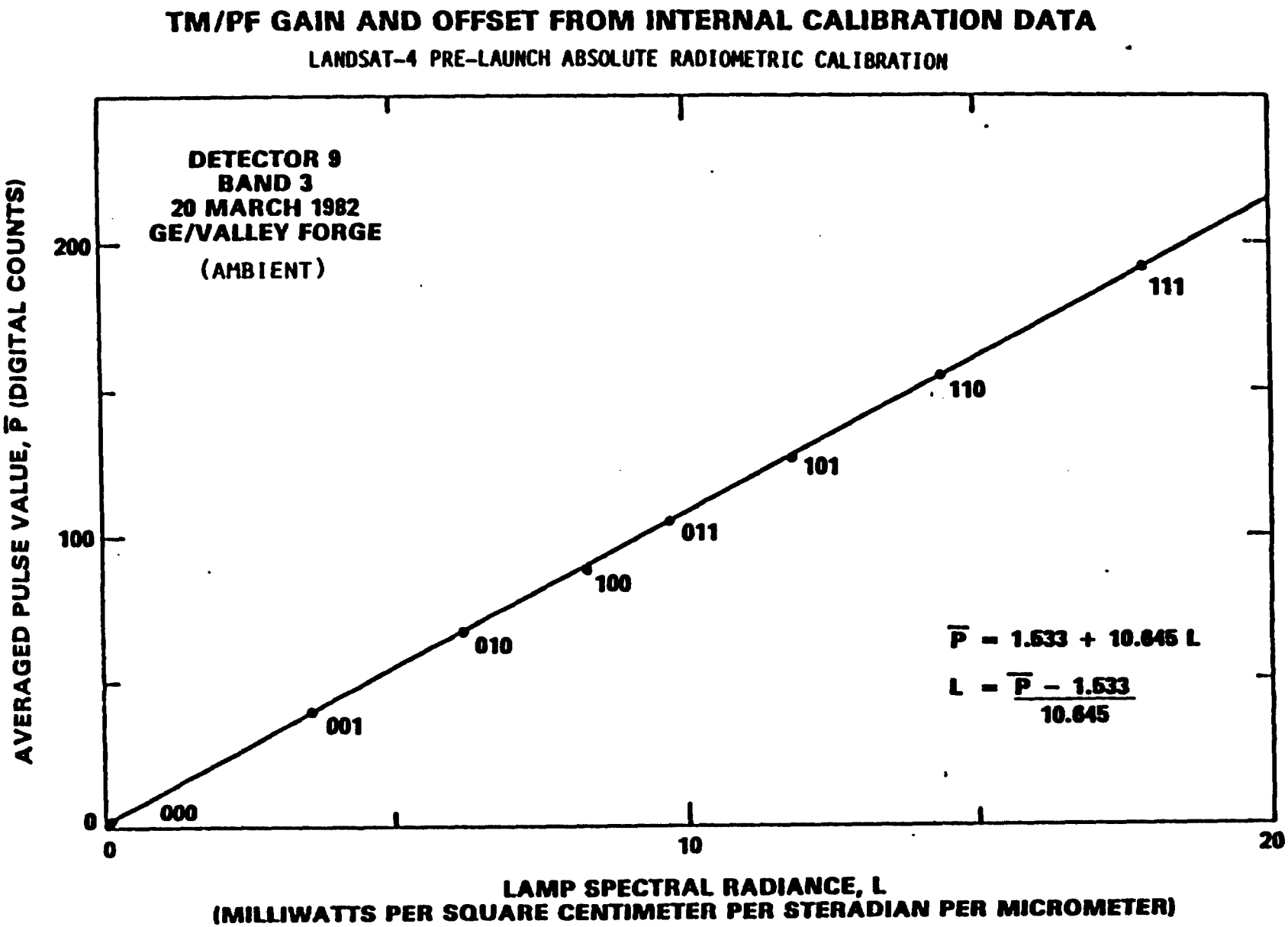

Figure 4. Landsat-4 TM Prelaunch Calibration Data for IC System.

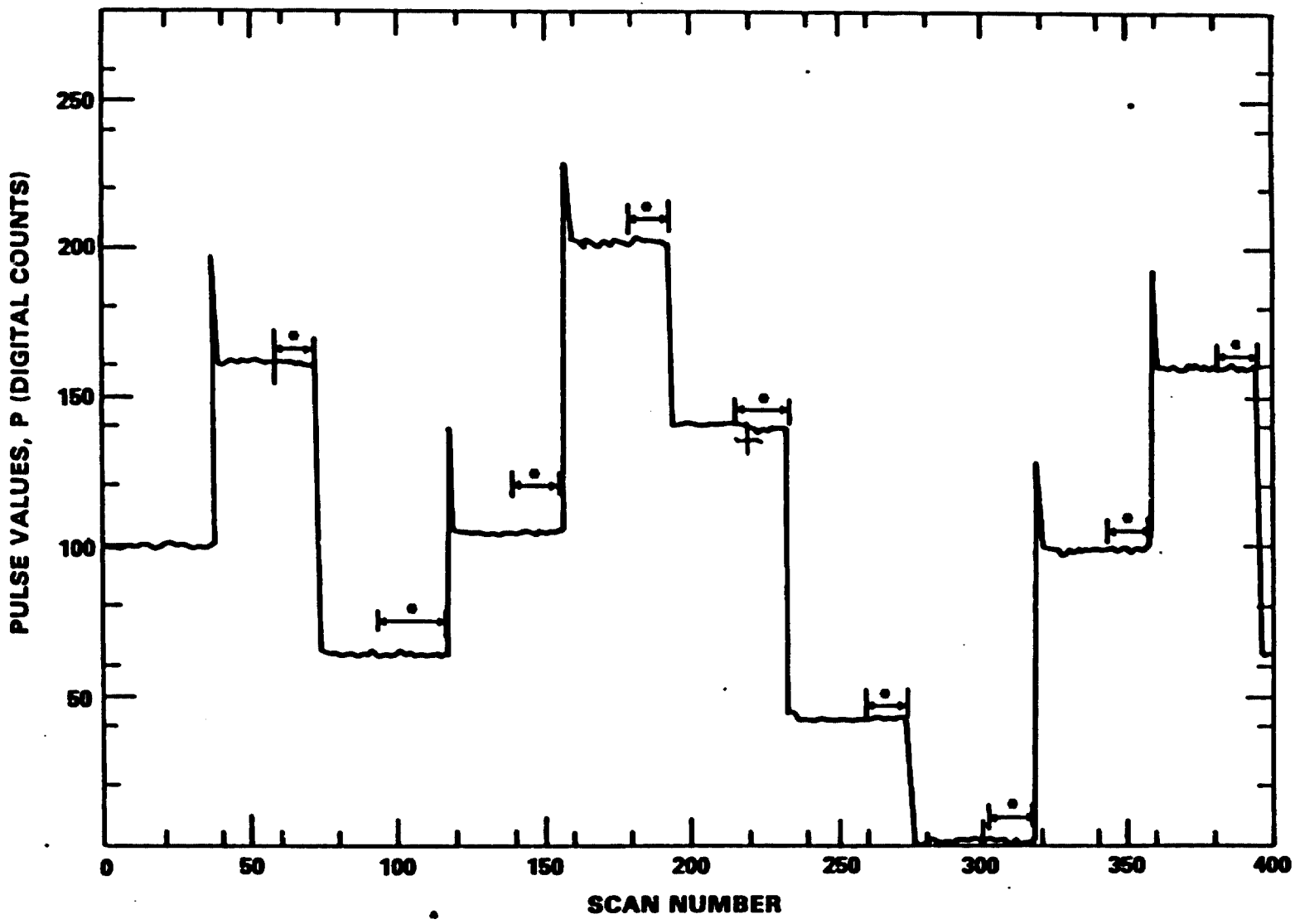

Figure 5. Landsat-4 TM in-orbit IC Calibration Data.

Radiometric Calibration – TM Landsat-4
"Hughes Algorithm"

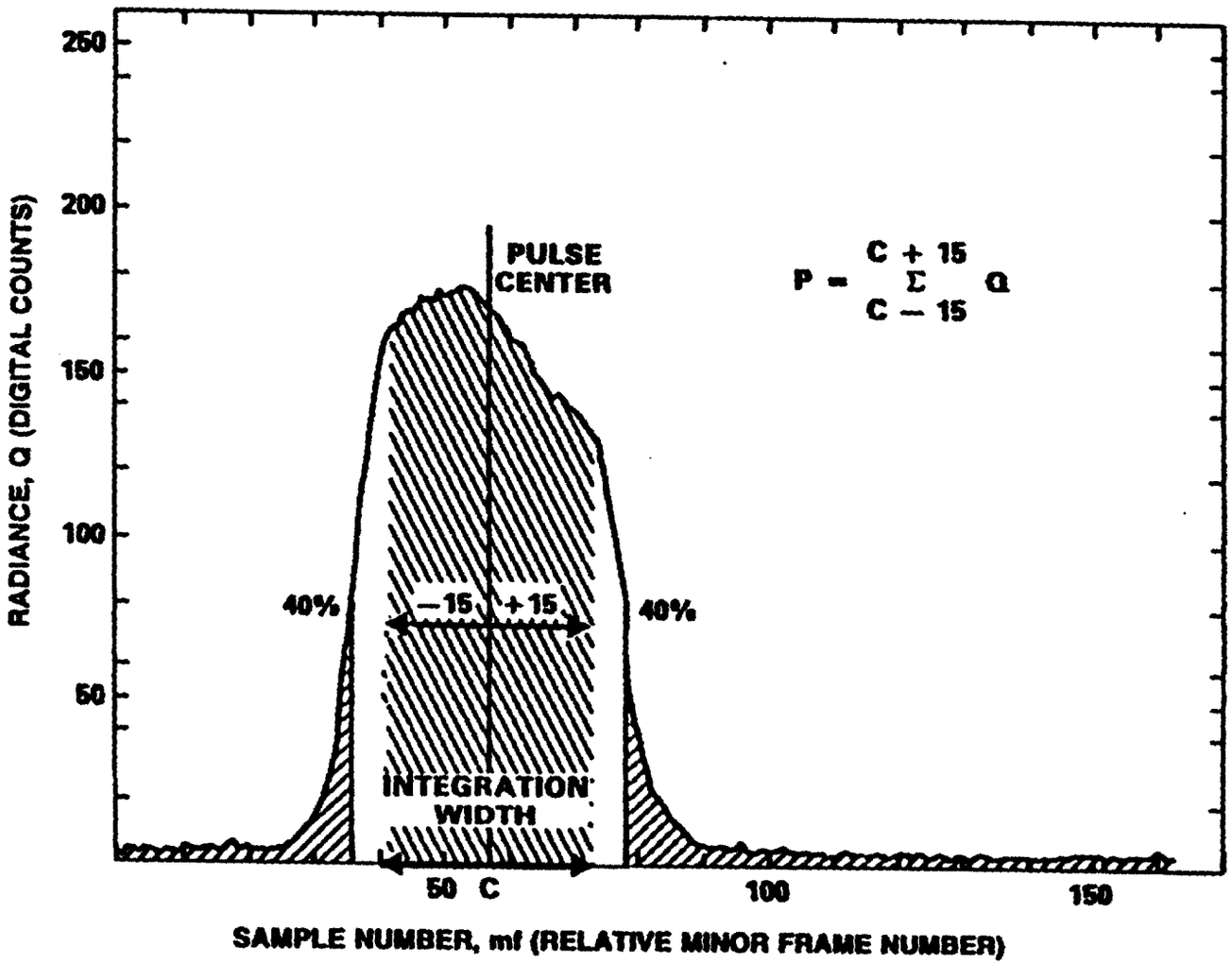

Figure 6. Landsat-4 TM IC Pulse Detail.

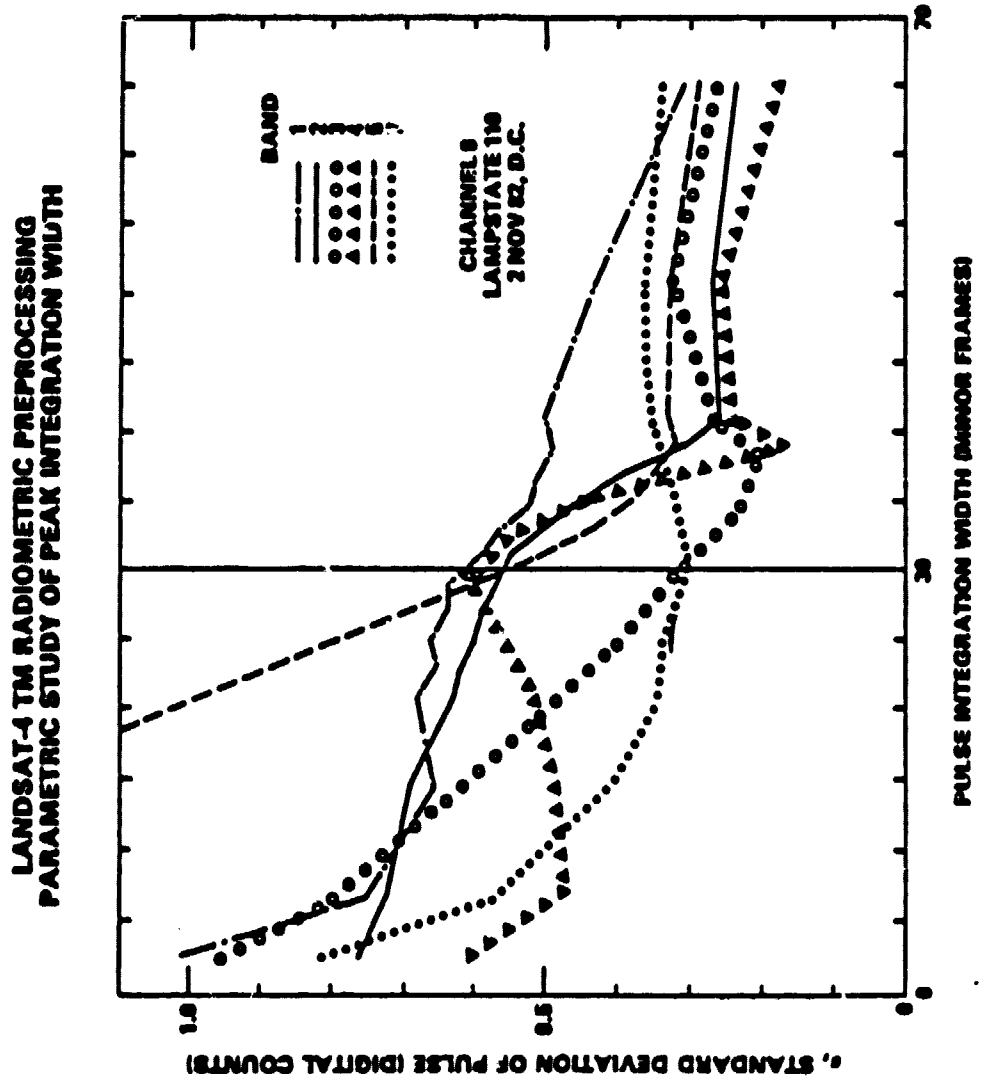

Figure 7. Landsat-4 TM IC Pulse Stability.

LANDSAT-4 TM RADIOMETRY

SCROUNGE-ERA GROUND PROCESSING OPTIONS

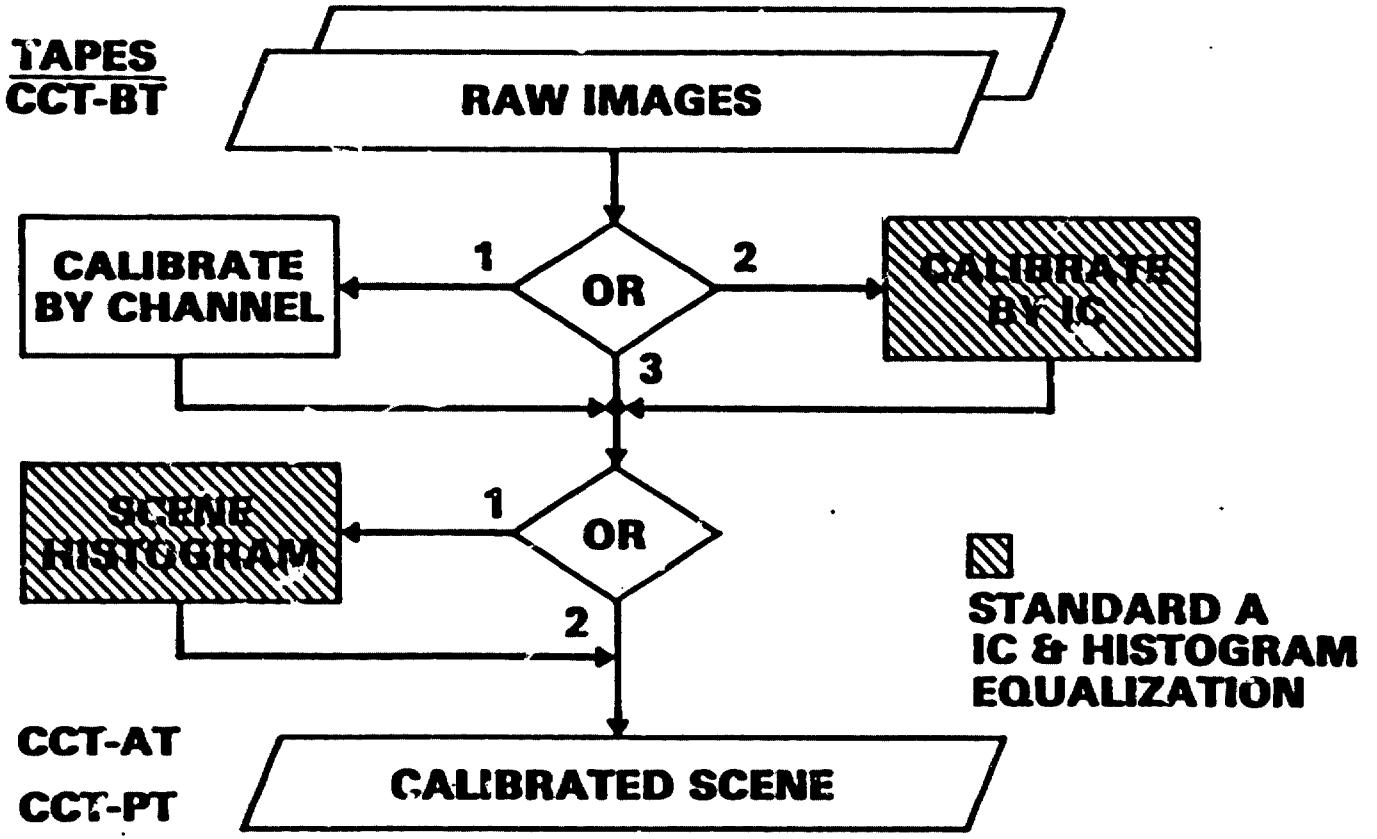

Figure 8. Standard and Optional Calibration Procedures (Barker et al., 1983c).

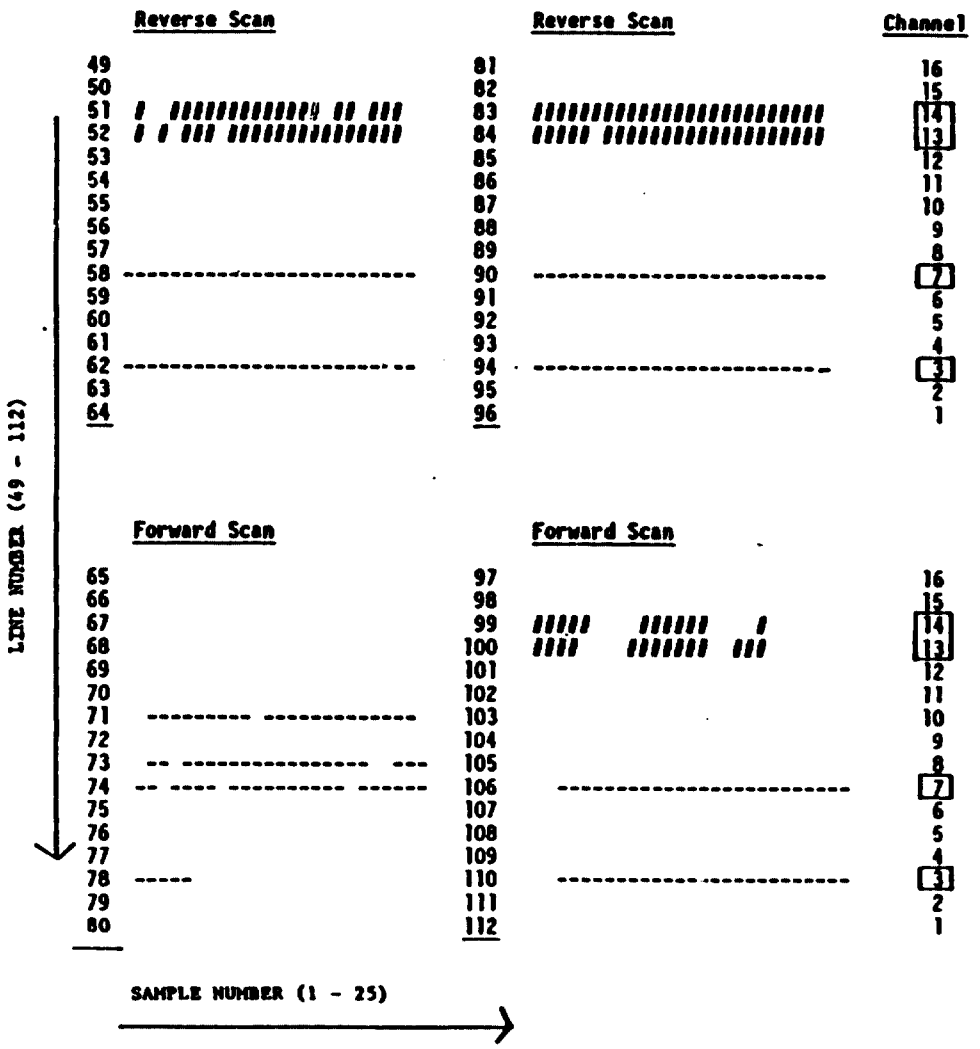

Figure 9. Landsat-4 TM Nominal-IC Difference Image. Blanks indicate no Difference.

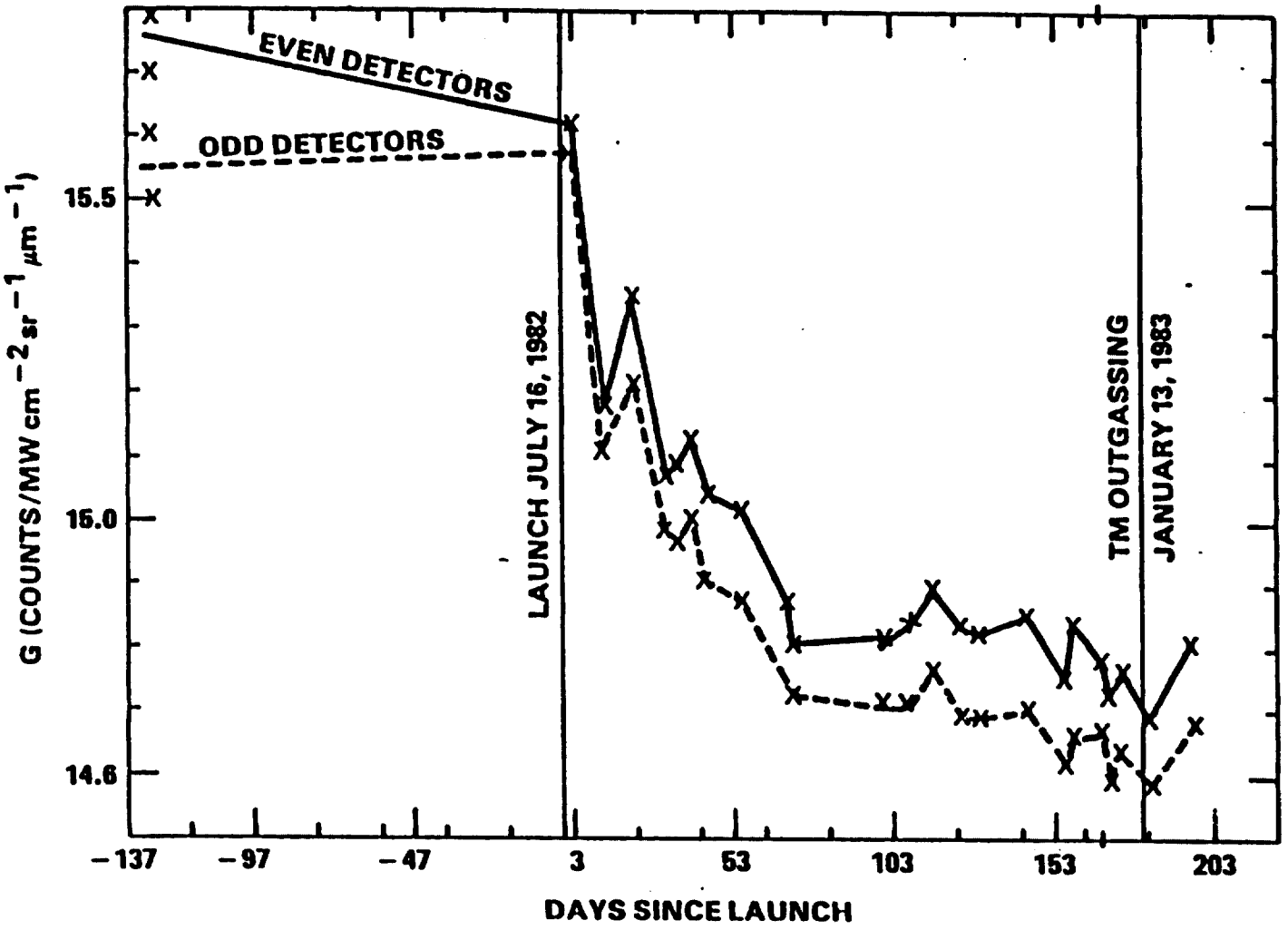

Figure 10. Exponential Change in Gain for TM PFP Band 1.

Thermal Band Gain Change with Time

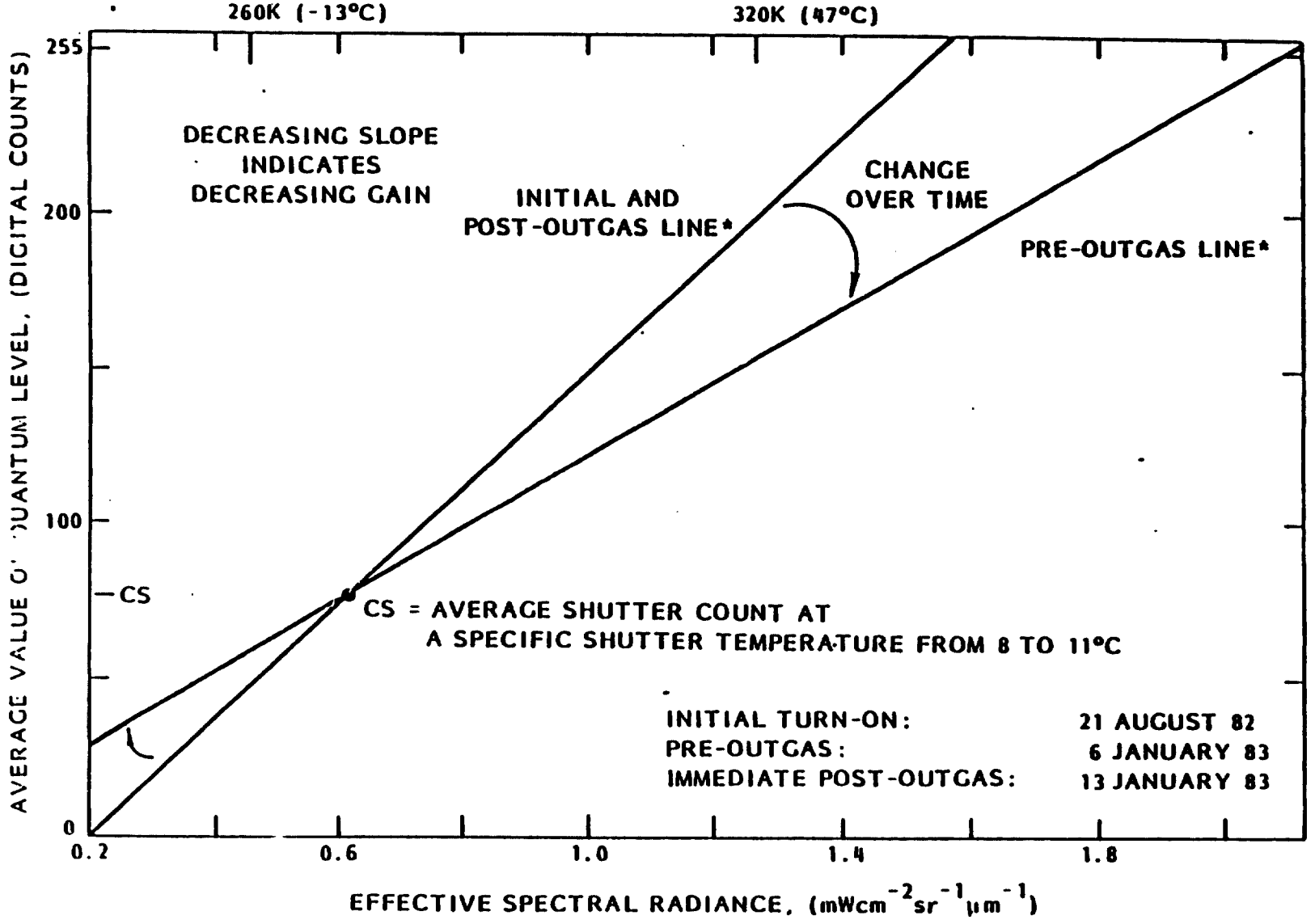

Figure 11. Thermal Band (Band 6) Change in Gain with Time.

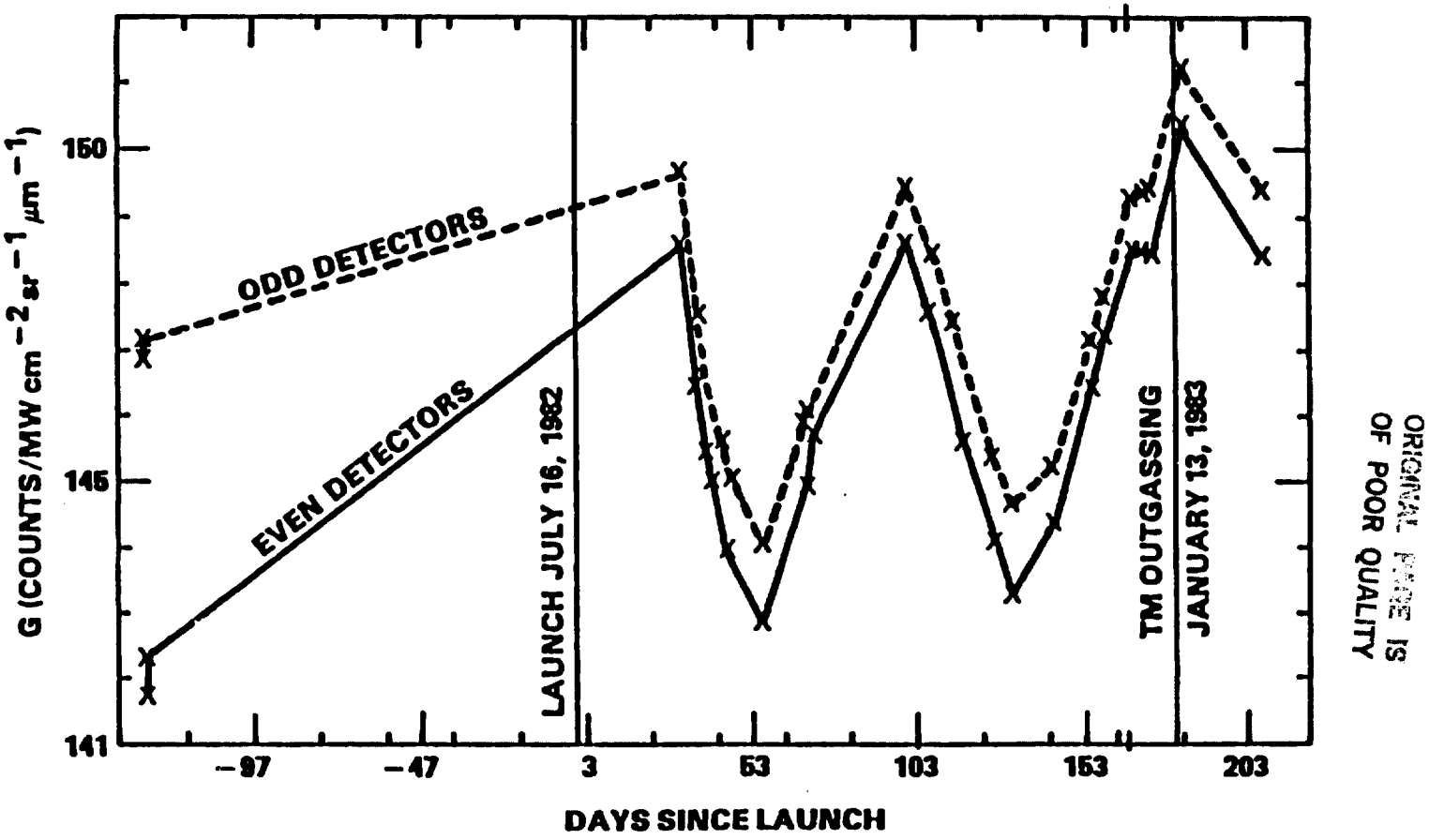

Figure 12. Gain Variability for Landsat-4 TM CFP (Band 7).

Ice (Solid Water) Half-Thickness

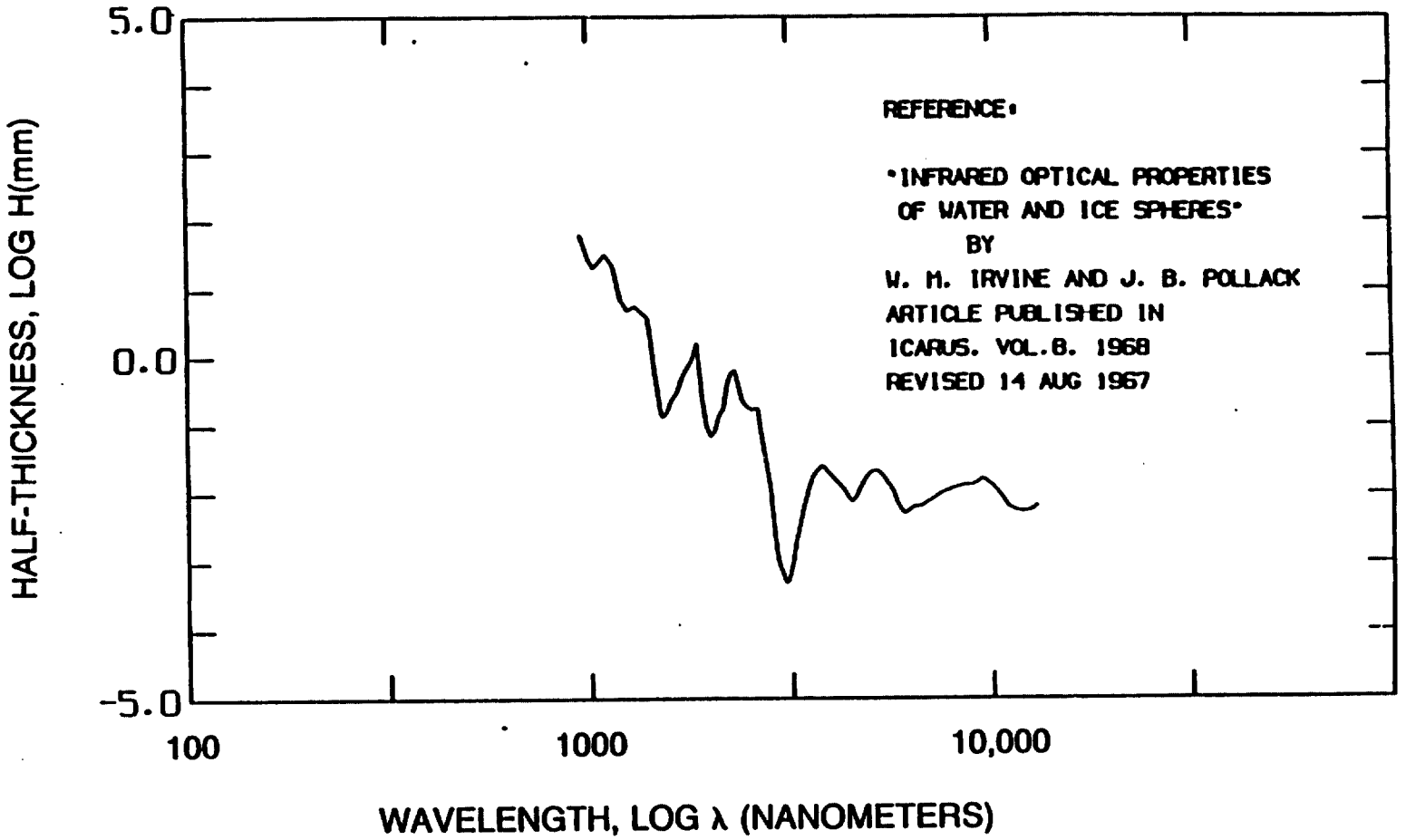

Figure 13. Ice Thickness needed to reduce Transparency by 50% at Infrared Wavelengths.

GODDARD SPACE FLIGHT CENTER
PURE PIXEL SAMPLING SITES

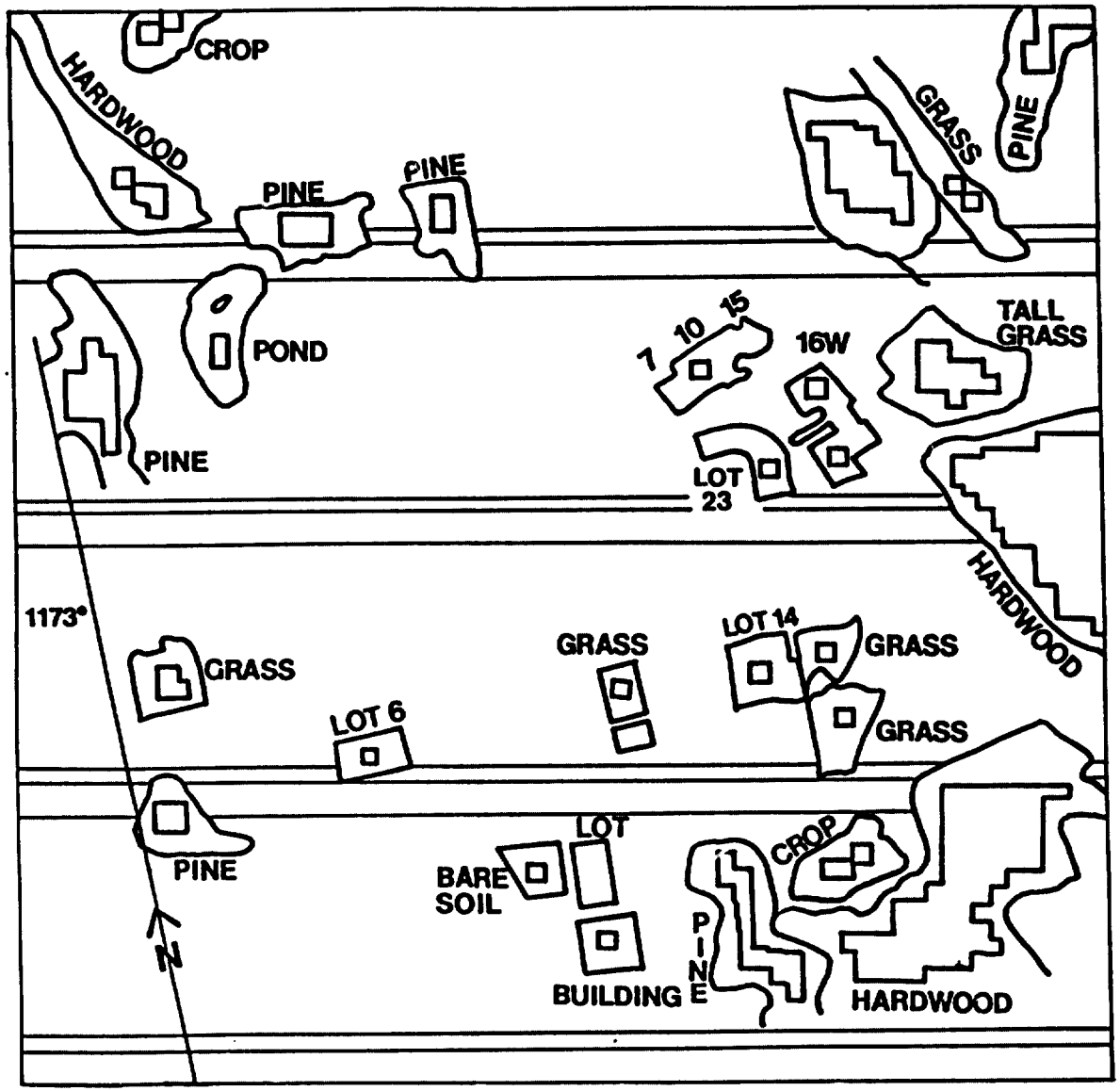

Figure 14. Apparently Pure Pixels for TM 64x64 Subimage of NASA/Goddard (Scene ID 40109-15140).

GODDARD SPACE FLIGHT CENTER BUILDINGS

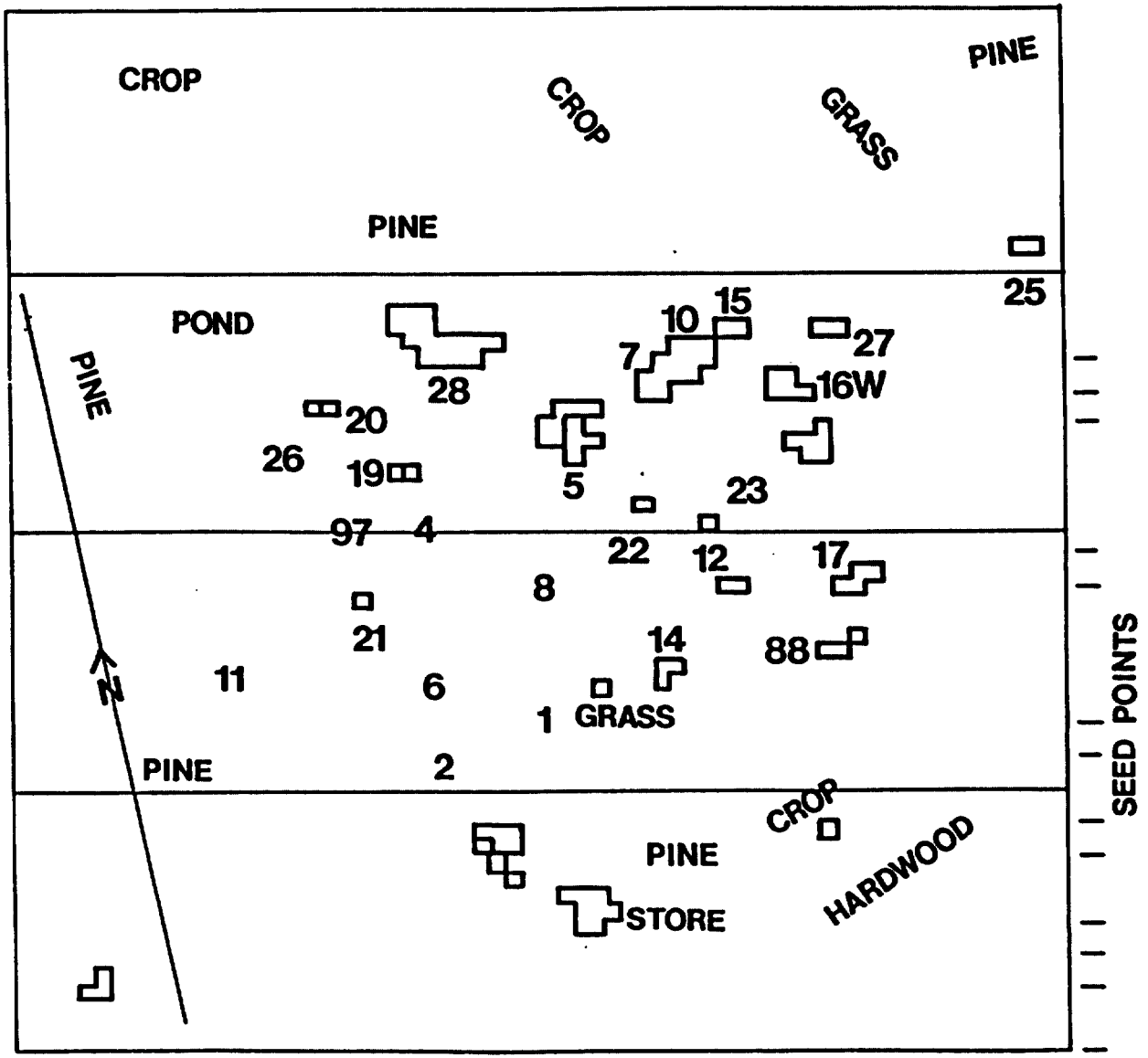

Figure 15. Building of NASA/Goddard Detected in TM Subscene.

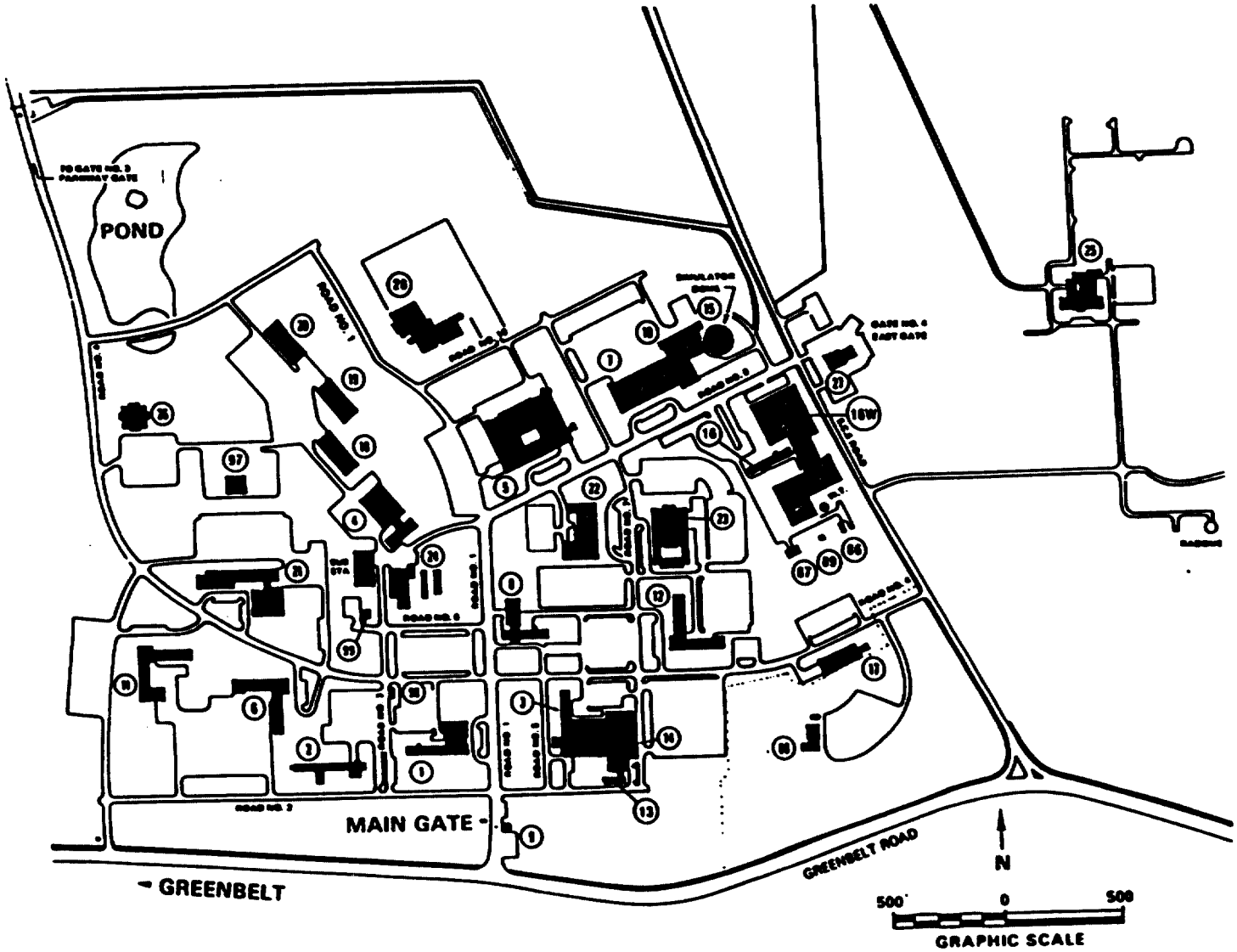

Figure 16. Ground-truth Map for Figures 14 and 15.